



PERGAMON

Available online at www.sciencedirect.com

 ScienceDirect

Acta Astronautica 60 (2007) 111–118

ACTA
ASTRONAUTICA

www.elsevier.com/locate/actaastro

Spatially explicit, nano-mechanical models of the muscle half-sarcomere: Implications for biomechanical tuning in atrophy and fatigue

Aya Kataoka^{a,1}, Bertrand C.W. Tanner^{b,1}, J. Michael Macpherson^c, Xiangrong Xu^d, Qi Wang^d, Michael Regnier^b, Thomas L. Daniel^e, P. Bryant Chase^{a,*}

^aDepartment of Biological Science and Program in Molecular Biophysics, Florida State University, Tallahassee, FL 32306, USA

^bDepartment of Bioengineering, University of Washington, Seattle, WA 98195, USA

^cDepartment of Biological Sciences, Stanford University, Stanford, CA 94305, USA

^dDepartment of Mathematics, Florida State University, Tallahassee, FL 32306, USA

^eDepartment of Biology, University of Washington, Seattle, WA 98195, USA

Received 18 May 2005; accepted 18 July 2006

Available online 9 October 2006

Abstract

Astronaut biomechanical performance depends on a wide variety of factors. Results from computational modelling suggest that muscle function—a key component of performance—could be modulated by compliance of the contractile filaments in muscle, especially when force is low such as transient Ca^{2+} activation in a twitch, reduced activation in muscle fatigue encountered during EVA, or perhaps atrophy during prolonged space flight. We used Monte-Carlo models to investigate the hypotheses that myofilament compliance influences muscle function during a twitch, and also modulates the effects of cooperative interactions between contractile proteins on force generation. Peak twitch force and the kinetics of force decay were both decreased, while tension cost was increased, when myofilament compliance was increased relative to physiological values. Both the apparent Ca^{2+} sensitivity and cooperativity of activation of steady-state isometric force were altered by myofilament compliance even when there were no explicit interactions included between binding sites. The effects of cooperative interactions between adjacent regulatory units were found to be greater than either the effect of myofilament compliance on apparent cooperativity of activation or that due to myosin cross-bridge-induced cooperativity. These results indicate that muscle function may be “tuned” at the molecular level, particularly under conditions of reduced Ca^{2+} activation.

© 2006 Published by Elsevier Ltd.

1. Introduction

Human biomechanical performance, in space and on Earth, depends on a wide variety of factors, both intrinsic and extrinsic to the work-performing muscles. Performance is affected acutely by factors internal to muscle such as changes in metabolite concentrations and Ca^{2+} release/uptake that contribute to muscle fatigue [1–7]. Over the long term, performance can be affected by changes in the quantity (e.g., atrophy)

¹ The first two authors (Kataoka and Tanner) made equal contributions.

* Corresponding author.

E-mail addresses: akataoka@sb.fsu.edu (A. Kataoka), bcwt@u.washington.edu (B.C.W. Tanner), macpher@stanford.edu (J.M. Macpherson), xxu@math.fsu.edu (X. Xu), wang@math.fsu.edu (Q. Wang), mregnier@u.washington.edu (M. Regnier), danielt@u.washington.edu (T.L. Daniel), chase@bio.fsu.edu (P.B. Chase).

and quality (e.g., fast versus slow muscle isoforms) of proteins in the myofilament lattice [8,9].

Performance can also be impacted, positively or negatively, by the material properties of tools and other objects and surfaces [10,11] that astronauts interact with. Numerical simulations are a crucial means for evaluating the significance of material properties—particularly compliance—of the protein filaments that constitute the microscopic structure of muscle and comprise the molecular mechanism of contraction [12–14]. Modelling indicates that altering compliance of the myofilament lattice—which is difficult to vary experimentally—can modulate steady isometric tension, and this modulation is greatest when the thin (actin) filaments of the sarcomere are less than fully activated by Ca^{2+} [12]. This molecular phenomenon parallels biomechanical “tuning” at the organismal level [10,11]. The modelling results further imply that modulation of force would be most significant during muscle twitch activity, during fatigue, when force and power output are depressed, and possibly also for atrophied muscle [15].

In this study, we extend our computational studies to investigate (i) the influence of myofilament compliance on twitch dynamics, and (ii) the interplay between myofilament compliance and cooperative activation of the thin filament. Our simulations indicate that (i) peak twitch force and the kinetics of force decay are both decreased, while tension cost is increased, when myofilament compliance is increased relative to physiological values, and that (ii) the activation dependence of isometric force appears to be affected less by cooperative effects of myosin cross-bridges on thin filament activation than by altered (reduced) filament compliance, although cooperative interactions along the thin filament have a greater influence than either.

2. Methods

2.1. Twitch modelling: multifilament model

Actin and myosin interactions produce force in the muscle [16]. In striated muscles, myosin and actin are present in thick and thin filaments, respectively. Ca^{2+} controls actin–myosin interactions through thin filament regulatory proteins troponin (Tn) and tropomyosin (Tm). Structurally, a thin filament regulatory unit (RU) consists of one Tn associated with one Tm and seven actin monomers [17]. Neuronal stimuli induce Ca^{2+} release from the sarcoplasmic reticulum (SR) into the myoplasm; a single stimulus results in a Ca^{2+} transient because released Ca^{2+} is actively transported back into

the SR [18]. Myoplasmic Ca^{2+} binding to Tn causes motion of the adjacent Tm and thus exposes myosin-binding sites, i.e., a portion of the actin monomers in an RU. Myosin molecules in the appropriate orientation can then form cross-bridges (XBs) by strong binding to actin, producing a contraction. Myofilament compliance alters the probability of myosin binding to available actin monomers through force-dependent changes in the spacing of myosin-binding sites on actin relative to the spacing of myosin in the thick filament [19,20]. We refer to this phenomenon as compliant realignment of binding (CRB) sites [13].

To test the prediction that CRB could modify twitch dynamics, we utilized a spatially explicit, Monte-Carlo model for the muscle half-sarcomere that consists of 13 thin filaments and three (half) thick filaments [12]. The three-state XB cycle (State 1 = unbound, State 2 = low force, weakly attached, and State 3 = high force, strongly attached; Fig. 1) and two states of an RU (unavailable (off) and available (on) for XB binding; Fig. 1) were the same as described previously; transitions between all states were Monte-Carlo processes [12]. In this model, there was no explicit cooperativity between RUs [12]. Availability of myosin-binding sites on actin was described by an activation probability (P_a) which is formally equivalent to $[\text{Ca}^{2+}]k_{\text{on}}/k_{\text{off}}$ (Fig. 1).

To simulate Ca^{2+} transients, the time-dependent single twitch activation probability ($P_a(t)$) was generated using the following equations that were based in part on

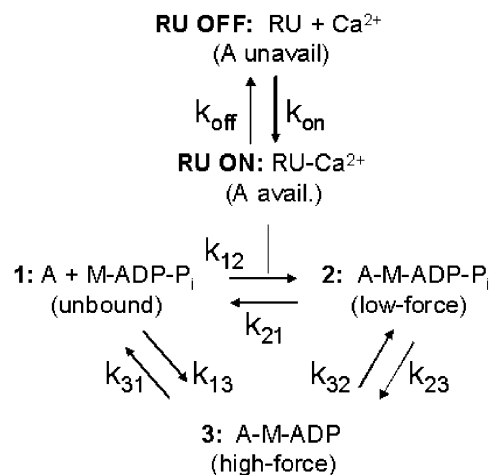


Fig. 1. Model kinetics. Thin filament regulatory unit (RU) kinetics are Ca^{2+} dependent and binary, such that RU_{off} or RU_{on} makes an actin site unavailable or available, respectively, for myosin binding. The cross-bridge cycle is the same as described [13] with the exception that the forward transition of actin and myosin binding (States 1–2) is constrained by requiring that there is a Ca^{2+} -activated, available actin.

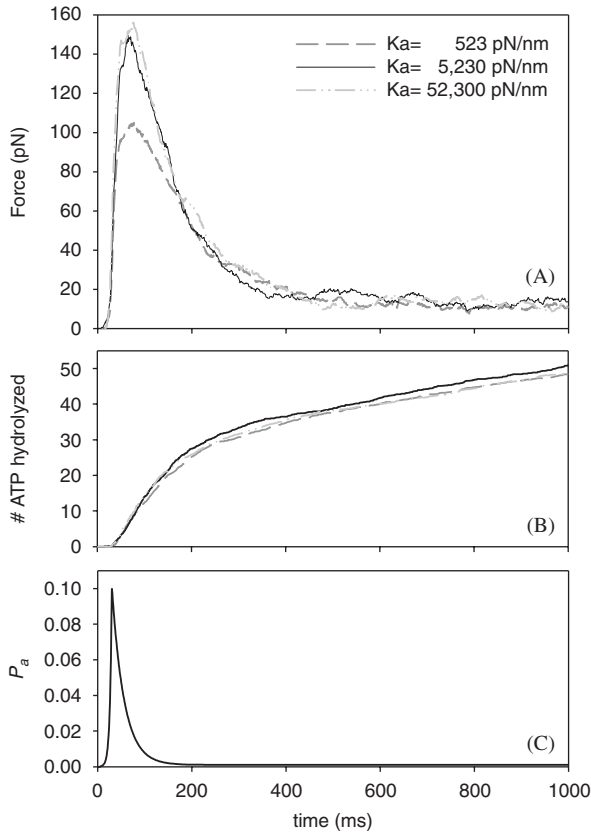


Fig. 2. Example simulations of single twitches using the multifilament model [12]. Average model (A) force and (B) cumulative ATP hydrolysis ($N = 15$) with actin filament stiffness $K_a = 10\%$, 100% or 1000% of that measured in frog skeletal muscle ($K_a = 5230 \text{ pN/nm}$ with a rest length $a_0 = 12.33 \text{ nm}$) [12,19,20], XB stiffness was 1 pN/nm . (C) Maximum activation probability (P_a) of 10% was used for these simulations. Note that peak force was substantially depressed with reduced K_a (increased filament compliance).

Ca^{2+} transients from rat flexor digitorum brevis fibers [21] (Fig. 2C).

$$P_a(t) = \begin{cases} 0; & t < 5 & \text{(a)} \\ \exp^{0.25(t-5)}/518; & 5 \leq t \leq 30 & \text{(b)} \\ (\exp^{-38.565(t-30)/1000}) + 0.0001; & t > 30 & \text{(c)} \end{cases} \quad (1)$$

There is an initial 5 ms delay (Eq. (1a)), after which $P_a(t)$ increases exponentially with a rate of 0.25 ms^{-1} and a scaling factor of $\frac{1}{518}$ (Eq. (1b)) which makes $P_a \approx 1$ at $t = 30 \text{ ms}$. For $t > 30 \text{ ms}$, $P_a(t)$ decreases exponentially with a rate of 38.565 s^{-1} (Eq. (1c)). The peak value of $P_a(t)$ in Eq. (1) is 1, that is, all RUs are activated. To obtain curves with submaximal peak values (30% , 10% , or 5% of maximum), Eq. (1) was multiplied by 0.3 , 0.1 , and 0.05 , respectively (Fig. 2C).

Each Monte-Carlo simulation corresponded to 1000 steps with step time (dt) of 1 ms . Fifteen simulations were run with each set of parameters. The initial value for stiffness of actin filaments (K_a ; note that stiffness is the inverse of compliance) was assigned to be equal to that measured in frog skeletal muscle (spring constant $K_a = 5230 \text{ pN nm}^{-1}$ and a rest length $a_0 = 12.33 \text{ nm}$) [19,20]. ATP hydrolysis was evaluated by equating one ATP hydrolyzed for each cross-bridge transition from the strongly attached to the detached state.

Analysis: The result of first $65\text{--}75 \text{ ms}$ of each 1000 ms simulation of force development was fit using nonlinear least-square regression (SigmaPlot ver. 8.0, SPSS Inc.) to a three-parameter Chapman equation:

$$F(t) = a(1 - \exp^{-bt})^c. \quad (2)$$

Due to the variability in exponent c , the half-time ($t_{1/2}$) for the tension rise was determined using this equation, and then the apparent rate of tension rise was calculated according to

$$\frac{-\ln 0.5}{t_{1/2}}. \quad (3)$$

The tension decay portion of each simulation ($65\text{--}75 \text{ ms}\text{--}1000 \text{ ms}$) was fit using nonlinear least-square regression to a three-parameter exponential decay function:

$$F(t) = F_0 + a(e^{-kt}), \quad (4)$$

where k is the rate of tension decay.

2.2. Thin filament RU cooperativity modelling: two-filament model

Our second goal of this study was to compare the effects of various types of cooperative interactions between myofilament proteins on force production using a model that has compliant filaments.

Under constant intracellular $[\text{Ca}^{2+}]$, force reaches an average steady-state value (F). Experiments using demembrated muscle fibers show a sigmoidal variation in F with respect to pCa ($\text{pCa} = -\log_{10}[\text{Ca}^{2+}]$, where $[\text{Ca}^{2+}]$ is in molar):

$$\frac{F}{F_{\max}} = \frac{1}{1 + 10^{n(\text{pCa} - \text{pCa}_{50})}}. \quad (5)$$

In Eq. (5), pCa_{50} is the pCa at which $F/F_{\max} = 0.5$ and is a measure of Ca^{2+} sensitivity. Parameter n is the slope of this force– pCa relationship around pCa_{50} , and is a measure of cooperativity; $n > 1$ suggests there are cooperative processes that influence force

production. The molecular mechanisms responsible for cooperativity in muscle allow for rapid and greater force production over a small change in intracellular $[Ca^{2+}]$.

Mechanisms of cooperativity may arise through (i) neighboring RUs, when a Ca^{2+} -activated RU increases the likelihood of adjacent RU activation through interactions between overlapping Tm molecules (termed RURU cooperativity); (ii) strongly bound, high-force bearing myosin heads in Ca^{2+} -activated RUs increasing the likelihood of adjacent RU activation through a myosin-induced displacement of the Tm that is translated along neighboring Tms (termed XBRU cooperativity); and (iii) strongly bound, high-force bearing myosin heads that increase the probability of neighboring myosin binding via a favorable realignment of the compliant myofibril lattice (termed XBXB cooperativity) [13,17,22]. Each mechanism of cooperativity has an inherent spatial component that must be addressed when investigating cooperative contributions to force production. Our modelling platform [12,13] allows us to examine the effects of each cooperative mechanism independently to see whether one has a dominant influence on force production.

Kinetics of Ca^{2+} regulation: Because this portion of the modelling adds several new parameters, described in detail below, we utilized a single actin filament interacting with a single myosin filament to reduce computational complexity and thus time, as described earlier [13,14]. As described above, the Ca^{2+} regulatory scheme that controls availability of an actin site for binding a proximal myosin head can take on either of two states, available or unavailable. We now introduce kinetics for transitions between these two states, with a Ca^{2+} association equilibrium $K_{eq} = k_{on}/k_{off} = 10^6 M^{-1}$, where k_{on} and k_{off} are the Ca^{2+} on and off rates from Tn, respectively, convolved with conformational changes in the RU (Fig. 1). k_{off} was set to $0.2 s^{-1}$, and k_{on} becomes the product of K_{eq} and k_{off} . As above, the simulation uses Monte-Carlo stochastics with a time step, $dt = 1 ms$. The transition probability of activating a RU (p_f) and making an actin site available for myosin binding becomes $p_f = k_{on}[Ca^{2+}]dt$. Whether an actin site is available to bind affects the cross-bridge cycle at the unbound to bound transition (States 1–2 in Fig. 1).

Cooperative feedback: We simulate increased activation (i.e., greater exposure of myosin-binding sites on actin) of a RU in either RURU or XBRU cooperativity by increasing p_f by the scalar multiplier m , where m is our feedback factor. In these simulations m was set to 100. m affects p_f when a neighboring actin site is available to bind myosin (RURU cooperativity), or

a high-force bearing myosin head is strongly bound to the site (XBRU cooperativity). Simulating both RURU and XBRU cooperative feedback combines each type of cooperativity, such that p_f increases by m whether any neighboring actin site is available for binding or is occupied by a strongly bound, high-force bearing myosin head. The XBXB cooperativity is innately built into the model through filament compliance. The simulations for XBXB cooperativity modify both the thick and thin filaments by a scalar factor X , where X is set to either 10 or 0.1. This creates a stiffer or more compliant filament lattice, respectively, without drastically exceeding the range of reported values for lattice stiffness.

For the two-filament geometry used in this portion of the modelling, the fraction of actin sites available is directly proportional to the number of RUs that are Ca^{2+} -activated (RU_{on}). RU_{on} is defined in time (t) by the differential equation:

$$\frac{dRU_{on}}{dt} = k_{off}\{K_{eq}[Ca^{2+}] - RU_{on}(1 + K_{eq}[Ca^{2+}])\}, \quad (6)$$

which has the analytical solution

$$RU_{on}(t) = RU_{on}(\infty)\{1 - e^{-t/\tau_{Ca}}\}, \quad (7)$$

where $RU_{on}(\infty)$ is the value of $RU_{on}(t)$ as $t \rightarrow \infty$ and τ_{Ca} is the time constant for RU_{on} development. The explicit parameters for $RU_{on}(\infty)$ and τ_{Ca} are:

$$RU_{on}(\infty) = \frac{K_{eq}[Ca^{2+}]}{1 + K_{eq}[Ca^{2+}]} \quad (8)$$

and

$$\tau_{Ca} = \frac{1}{k_{off}(1 + K_{eq}[Ca^{2+}])}. \quad (9)$$

To be conservative, we used simulation durations that lasted $5\tau_{Ca}$ s, which provides enough time-steps for the thin filament to reach greater than 95% of the final, steady activation level. Based on our past simulations [13], we found that 40,000 data points provided sufficient numeric accuracy for calculations of F and its standard deviation. To accomplish this, we varied the number of runs for each $[Ca^{2+}]$ such that we (i) satisfy the simulation duration outlined above, and (ii) assure that we gather no fewer than 40,000 samples from the last 10% of each simulation to calculate F .

3. Results

3.1. Effects of filament compliance on Ca^{2+} -activated twitches: multifilament model

Averages of 15 simulations of twitch force and ATP hydrolysis during a Ca^{2+} transient (Eq. (1)) are shown in Fig. 2 for the multifilament model (Methods). Peak P_a for the Ca^{2+} transient was 0.1 in the records shown. Results from simulations using three values of K_a are shown: 5230 pN/nm (100% of physiological for the multifilament model); 52,300 pN/nm (1000% of physiological); and 523 pN/nm (10% of physiological). For the latter, which corresponds to increased filament compliance (compliance being the inverse of stiffness), peak force was decreased by 30% relative to physiological stiffness values while cumulative ATP hydrolysis was essentially unchanged.

Twitch simulations equivalent to those shown in Fig. 2 were obtained using as input Ca^{2+} transients (Eq. (1)) with peak P_a over the range of 0.05–1.0 (Methods). Peak twitch force was lower at all values of peak P_a with $K_a = 10\%$ of physiological (high filament compliance) compared with higher values of K_a (Fig. 3A), which is qualitatively consistent with decreased Ca^{2+} sensitivity of steady-state force when filament compliance is increased (decreased K_a) in the multifilament model [12]. Fig. 3B shows that there was no significant effect of twitch amplitude on tension cost. Tension cost increased, however, at all twitch amplitudes when filament compliance increased. As implied by the simulations in Fig. 2, this increase in tension cost is primarily due to the overall decrease in tension when K_a was decreased. Thus, filament compliance can modulate not only the mechanics, but also the energetics of muscle [14].

The kinetics of twitch tension rise and decay, analyzed as described in Methods, are shown in Fig. 4. There was little or no effect of filament compliance (or, conversely, K_a) on the rate of tension rise (Fig. 4A). The rate of tension rise exhibited a slight increase as the amplitude of the Ca^{2+} transient was increased (Fig. 4A). An increased rate of tension rise with increased Ca^{2+} is expected, based on steady-state Ca^{2+} data and modelling [12,23,24] although both the extent of increase with Ca^{2+} activation level and the effect of filament compliance were less than anticipated. Careful analysis of the model output showed that the rate of tension rise was dominated by the kinetics of the Ca^{2+} transient, which is of course not a consideration for conditions with steady Ca^{2+} levels.

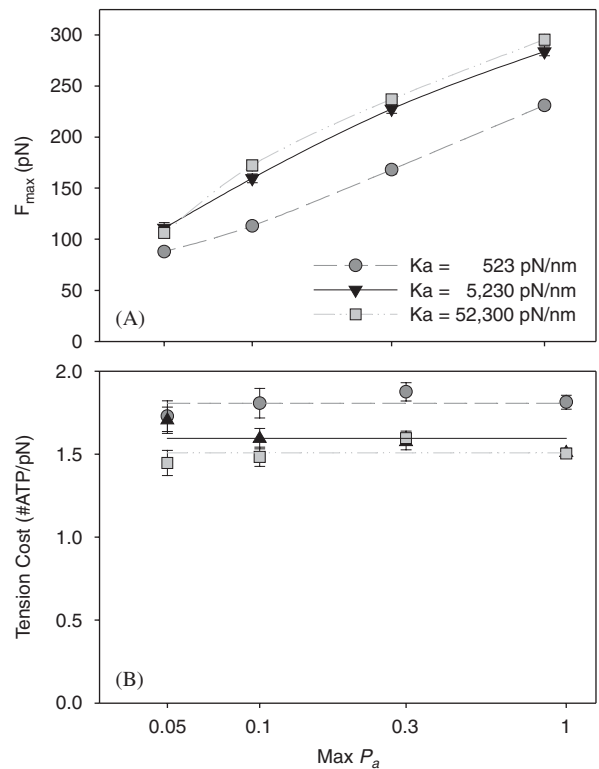


Fig. 3. Analysis of twitch (A) peak force and (B) tension cost. Each point represents the average of 15 simulations (as shown in Fig. 2) and error bars represent S.E. (A) Each averaged force for $K_a = 523$ pN is significantly different ($P < 0.05$) from the other two points at the same maximum P_a value. (B) Tension cost was calculated by dividing the total number of ATP hydrolyzed by the area under the force–time curve (Fig. 2A). Lines represent the mean tension cost for each value of K_a , which are significantly different from each other ($P < 0.05$).

The rate of twitch tension decay was not significantly affected by amplitude of the Ca^{2+} transient, but was significantly decreased when K_a was reduced to 10% of physiological (or, equivalently, when filament compliance was increased) at all levels of peak P_a (Fig. 4B).

3.2. Effects of thin filament RU cooperative interactions on steady-state isometric force: two-filament model

Simulations of force over time show that unregulated (all actin sites available) force reached 17.4 pN in the two-filament model (Methods), with a time constant of force development (τ_F) ~ 6 ms. This steady-state F for unregulated filaments was used as the normalization factor for all subsequent simulations (Fig. 5A). In simulations with regulated thin filaments, steady-state F increased with increasing $[\text{Ca}^{2+}]$ and the rate of force development increased (conversely, τ_F decreased;

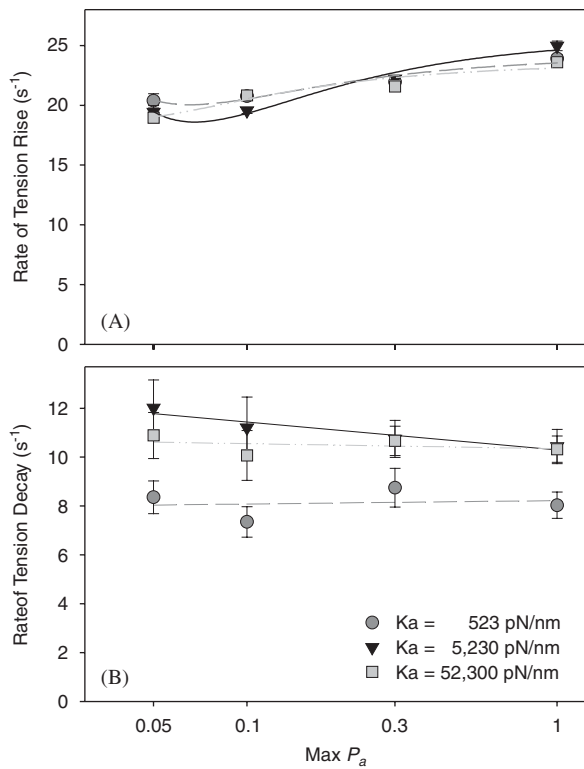


Fig. 4. Kinetic parameters of single twitch simulations. Rate of (A) tension rise and (B) tension decay were calculated as described in Methods. Points are the average \pm S.E. ($N = 15$). Lines represent (A) second-order polynomial fits, or (B) linear regressions for each value of K_a . The slopes in panel B are not significantly different from zero.

Fig. 5). The basal parameter set without any cooperative feedback yielded $n = 1.43$ and $pCa_{50} = 6.45$ (Figs. 5B and 6) when fit with the Hill equation (Eq. (5)). While the current model produces a somewhat greater Ca^{2+} sensitivity of force regulation (pCa_{50}) than values reported in the literature for skeletal muscle fibers, the sigmoidal relationship between pCa and F , and the Ca^{2+} dependence of the rate of force development simulate experimental results in fibers quite well [17,23,24]. The parameter n (Eq. (5)) is expected to be close to 1 in simulations without any cooperative feedback. We also observed that the standard deviation of steady-state F increased as $[Ca^{2+}]$ decreased (pCa increased). This is because fewer force-producing events occur at lower levels of $[Ca^{2+}]$, such that each incident has an increased relative contribution to simulated force at low $[Ca^{2+}]$.

Simulations of cooperative feedback (Fig. 6) suggest that the myofilament lattice is slightly more sensitive to RURU cooperativity than the other forms of

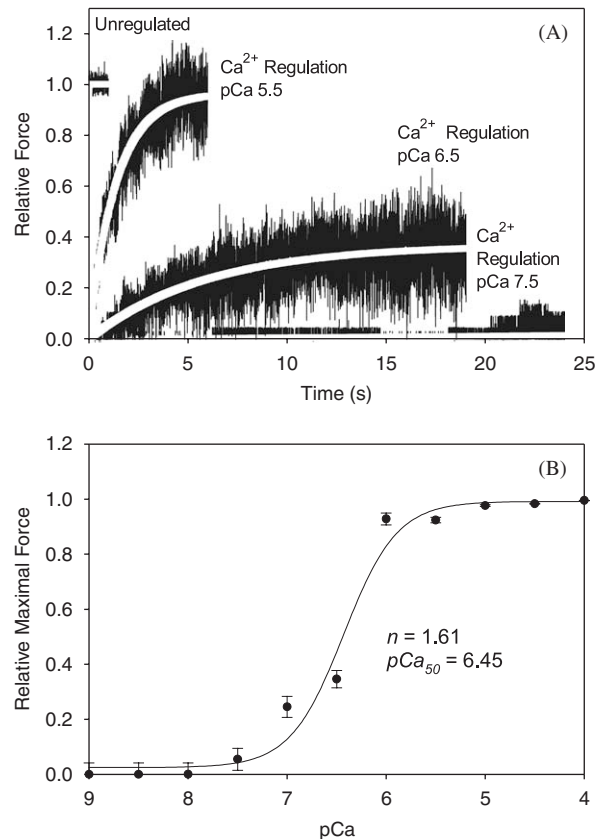


Fig. 5. Ca^{2+} -regulation of force in the two-filament model. (A) The mean force over a single run (black lines) for unregulated and a subset of Ca^{2+} -regulated (pCa levels 7.5, 6.5, 5.5) simulations. All force traces are normalized to the unregulated, steady-state F (17.4 pN). XB stiffness was 5 pN/nm. Force traces were fit using a rising exponential function (thick white line) $F(t) = F_{ss}(1 - \exp(-t/\tau_F))$, where $F(t)$ is force as a function of time, F_{ss} is the steady-state value of F , and τ_F is the time constant of force development. (B) Ca^{2+} -regulated F_{ss} as a function of pCa . Error bars on the data are S.D. of 40,000 time steps used to calculate F_{ss} . The line is the nonlinear least-squares regression on the Hill equation (Eq. (5)).

cooperativity. RURU cooperativity also has a dramatic influence on pCa_{50} that is not seen in the XBRU or XBxB simulations. XBRU cooperativity, however, appears to increase force production at low $[Ca^{2+}]$ and its contribution is diminished at higher $[Ca^{2+}]$. This suggests that XBs have a greater influence on force production when the thin filament is less activated, i.e., at submaximal pCa levels. The minimal contribution from XBRU cooperativity may result from small numbers of XBs bound to actin. With cooperative feedback (basal), the number of myosin heads bearing a high level of force does not exceed two or three, which translates into 10–15% of the population. Numerically, this low population of bound cross-bridges may be biasing our XBRU

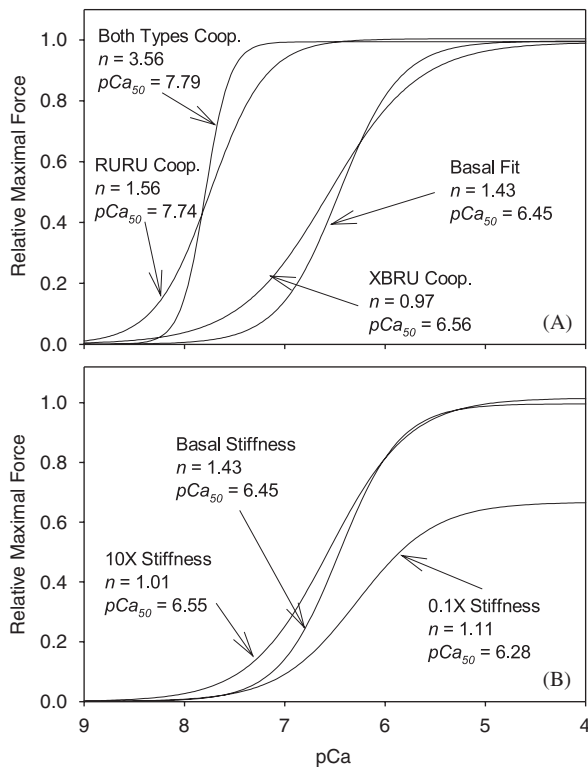


Fig. 6. Cooperative contributions to the steady-state isometric force–pCa relationship are shown using Hill fits (Eq. (5)) to each simulation (data are similar to that of Fig. 5). Each panel shows lines for basal regulation (no cooperative interactions) as well as cooperativity in the form of: (A) RURU, XBRU, and the combination of both RURU and XBRU; or (B) XBXB cooperativity by varying compliance of both the thick and thin filament.

cooperativity results in comparison with RURU cooperativity because there is always higher population of activated RUs (which approaches 100% above pCa 6). Interestingly, the simulations containing both RURU and XBRU cooperativity appear to have a synergistic effect on n , suggesting that it requires more than one form of cooperativity to approach the n values (3–6) most often reported in the literature [17]. Simulations of XBXB cooperativity appear to have little effect on n , however there are some shifts (ΔpCa_{50}) in the F –pCa relationship. This is greatest in the more compliant filament lattice, where the slope (n), Ca^{2+} sensitivity (pCa_{50}), and F are damped from the basal level. Force production in the simulation with $K_a = 1000\%$ physiological values shows that increased lattice stiffness increases force production at lower $[Ca^{2+}]$ levels.

4. Discussion

Taken together, the results of this modelling study suggest that increases in compliance (decreases in

stiffness) of the myofilaments in a muscle sarcomere have the potential to substantially alter contractile performance, and confirm that the greatest effects would occur at low force levels. Physiologically, the twitch simulations demonstrate that aspects of magnitude, energetics, and kinetics of force production may all be affected by the fact that myofilaments are not infinitely rigid. This suggests that aspects of muscle function may be “tuned” at the level of protein mechanics, just as biomechanical performance may be “tuned” by the external environment [10,11].

4.1. Filament compliance and cooperative activation of the thin filament

The physiological representation of the myofilament lattice and the multidirectional force between the filaments is improved in the multifilament model (Figs. 3 and 4) [12] from the earlier two-filament model [13]. However, for computational simplicity we reverted to the two-filament model for this investigation of Ca^{2+} -regulation and cooperative activation of force production (Figs. 5 and 6). This was done to improve upon our earlier models by explicitly requiring the availability of each myosin-binding site on actin to depend on $[Ca^{2+}]$ and the Ca^{2+} -binding kinetics of Tn, in addition to introducing different forms of cooperative thin–thick filament interactions. Understanding the impact of these model improvements on force between two filaments is a necessary precursor to understanding their influence in the more complex multifilament model system. We simulated cooperativity by increasing the activation probability of a RU (Methods; Fig. 1). Our simulations suggest that RURU cooperativity has a greater influence on Ca^{2+} -sensitivity of force development and a slightly greater effect on the cooperativity in the system (Fig. 6). However, the greatest increase in cooperative force production arises from a synergistic contribution from both RURU and XBRU cooperativity (Fig. 6).

4.2. Implications for manned space flight

Our simulations of muscle biomechanics at the level of assemblies of hundreds of macromolecules are being constructed as a component of the digital astronaut, a central tool for the health and well-being of humans during long-term space flight [25,26]. Our first long-term goal is to incorporate sufficient knowledge into the model to make it physiologically and biophysically accurate so that we can test novel physiological circumstances encountered in muscles undergoing atrophy (e.g., during prolonged space flight) or

hypertrophy (e.g., in response to exercise). The spatially explicit, macromolecular model is uniquely suited for computational investigation of muscles that contain multiple protein isoforms [8] or sarcomeres that have variable filament lengths [9]. This goal is important for using simulations in conjunction with experiments to evaluate potential countermeasures against muscle atrophy. Secondly, we anticipate that multiscale modelling approaches will be useful for achieving the additional goal of capturing key features of the detailed macromolecular model for simulations of whole muscles or groups of muscles, while gaining substantial reduction in the time required for simulations of higher order physiological systems.

Acknowledgments

A. Kataoka and B.C.W. Tanner contributed equally to this work. Support was from the US National Aeronautics and Space Administration (NASA) and the National Space Biomedical Research Institute (NSBRI) Grant MA00211.

References

- [1] P.B. Chase, M.J. Kushmerick, Effect of physiological ADP levels on contraction of single skinned fibers from rabbit fast and slow muscles, *American Journal of Physiology* 268 (1995) C480–C489.
- [2] P.B. Chase, M.J. Kushmerick, Effects of pH on contraction of rabbit fast and slow skeletal muscle fibers, *Biophysical Journal* 53 (1988) 935–946.
- [3] C. Karatzaferi, K.H. Myburgh, M.K. Chinn, K. Franks-Skiba, R. Cooke, Effect of an ADP analog on isometric force and ATPase activity of active muscle fibers, *American Journal of Physiology: Cell Physiology* 284 (2003) C816–C825.
- [4] W.A. Macdonald, D.G. Stephenson, Effects of ADP on action-potential induced force responses in mechanically skinned rat fast-twitch fibres, *Journal of Physiology* (2004) online preprint.
- [5] K.H. Myburgh, Can any metabolites partially alleviate fatigue manifestations at the cross-bridge?, *Medicine & Science in Sports & Exercise* 36 (2004) 20–27.
- [6] R. Vandenberg, The myofibrillar complex and fatigue: a review, *Canadian Journal of Applied Physiology* 29 (2004) 330–356.
- [7] R.W. Wiseman, T.W. Beck, P.B. Chase, Effect of intracellular pH on force development depends on temperature in intact skeletal muscle from mouse, *American Journal of Physiology: Cell Physiology* 271 (1996) C878–C886.
- [8] G.R. Adams, V.J. Caiozzo, K.M. Baldwin, Skeletal muscle unweighting: spaceflight and ground-based models, *Journal of Applied Physiology* 95 (2003) 2185–2201.
- [9] D.A. Riley, J.L. Bain, J.L. Thompson, R.H. Fitts, J.J. Widrick, S.W. Trappe, T.A. Trappe, D.L. Costill, Decreased thin filament density and length in human atrophic soleus muscle fibers after spaceflight, *Journal of Applied Physiology* 88 (2000) 567–572.
- [10] C.T. Farley, J. Glasheen, T.A. McMahon, Running springs: speed and animal size, *Journal of Experimental Biology* 185 (1993) 71–86.
- [11] T.A. McMahon, P.R. Greene, The influence of track compliance on running, *Journal of Biomechanics* 12 (1979) 893–904.
- [12] P.B. Chase, J.M. Macpherson, T.L. Daniel, A spatially explicit nano-mechanical model of the half-sarcomere: myofilament compliance affects Ca^{2+} -activation, *Annals of Biomedical Engineering* 32 (2004) 1559–1568.
- [13] T.L. Daniel, A.C. Trimble, P.B. Chase, Compliant realignment of binding sites in muscle: transient behavior and mechanical tuning, *Biophysical Journal* 74 (1998) 1611–1621.
- [14] T.L. Daniel, M.S. Tu, Animal movement, mechanical tuning and coupled systems, *Journal of Experimental Biology* 202 (Pt 23) (1999) 3415–3421.
- [15] D.R. Williams, The biomedical challenges of space flight, *Annual Review of Medicine* 54 (2003) 245–256.
- [16] R. Cooke, The sliding filament model: 1972–2004, *Journal of General Physiology* 123 (2004) 643–656.
- [17] A.M. Gordon, E. Homsher, M. Regnier, Regulation of contraction in striated muscle, *Physiological Reviews* 80 (2000) 853–924.
- [18] M.W. Berchtold, H. Brinkmeier, M. Müntener, Calcium ion in skeletal muscle: its crucial role for muscle function, plasticity, and disease, *Physiological Reviews* 80 (2000) 1215–1265.
- [19] H.E. Huxley, A. Stewart, H. Sosa, T. Irving, X-ray diffraction measurements of the extensibility of actin and myosin filaments in contracting muscle, *Biophysical Journal* 67 (1994) 2411–2421.
- [20] K. Wakabayashi, Y. Sugimoto, H. Tanaka, Y. Ueno, Y. Takezawa, Y. Amemiya, X-ray diffraction evidence for the extensibility of actin and myosin filaments during muscle contraction, *Biophysical Journal* 67 (1994) 2422–2435.
- [21] S.L. Carroll, M.G. Klein, M.F. Schneider, Decay of calcium transients after electrical stimulation in rat fast- and slow-twitch skeletal muscle fibres, *Journal of Physiology* 501 (Pt 3) (1997) 573–588.
- [22] M.V. Razumova, A.E. Bukatina, K.B. Campbell, Different myofilament nearest-neighbor interactions have distinctive effects on contractile behavior, *Biophysical Journal* 78 (2000) 3120–3137.
- [23] M. Regnier, A.J. Rivera, P.B. Chase, L.B. Smillie, M.M. Sorenson, Regulation of skeletal muscle tension redevelopment by troponin C constructs with different Ca^{2+} affinities, *Biophysical Journal* 76 (1999) 2664–2672.
- [24] M. Regnier, D.A. Martyn, P.B. Chase, Calcium regulation of tension redevelopment kinetics with 2-deoxy-ATP or low [ATP] in rabbit skeletal muscle, *Biophysical Journal* 74 (1998) 2005–2015.
- [25] R.J. White, J.B. Bassingthwaite, J.B. Charles, M.J. Kushmerick, D.J. Newman, Issues of exploration: human health and wellbeing during a mission to Mars, *Advances in Space Research* 31 (2003) 7–16.
- [26] R.J. White, M. Averner, Humans in space, *Nature* 409 (2001) 1115–1118.